

# Measuring Diffuse Neutrino Fluxes with IceCube

**Marek Kowalski**

Lawrence Berkeley National Laboratory  
Berkeley, CA, 94720, USA  
Email: MPKowalski@lbl.gov

**Abstract.**

In this paper the sensitivity of a future kilometer-sized neutrino detector to detect and measure the diffuse flux of high energy neutrinos is evaluated. Event rates in established detection channels, such as muon events from charged current  $\nu_\mu$  interactions or cascade events from  $\nu_e$  and  $\nu_\tau$  interaction, are calculated using a detailed Monte Carlo simulation. Neutrino fluxes as expected from prompt charm decay in the atmosphere or from astrophysical sources such as Active Galactic Nuclei (AGN) are modeled assuming power laws. The ability to measure the normalization and slope of these spectra is then analyzed.

It is found that the cascade channel generally has a high sensitivity for the detection and characterization of the diffuse flux, when compared to what is expected for the upgoing- and downgoing-muon channels. A flux at the level of the Waxman-Bahcall upper bound should be detectable in all channels separately while a combination of the information of the different channels will allow detection of a flux more than one order of magnitude lower. Neutrinos from the prompt decay of charmed mesons in the atmosphere should be detectable in future measurements for all but the lowest predictions.

PACS numbers: 14.60.Pqx,96.40.Tv,95.85.Ry

## 1. Introduction

High energy extra-terrestrial neutrinos have so far escaped their detection, and there is a considerable effort invested to change this situation soon [1]. IceCube, a Cherenkov detector with a volume of a cubic kilometer is currently being installed at the South Pole [2] and plans for a northern hemisphere detector of similar size are maturing [3]. Such detectors are expected to measure high energy neutrinos ( $E_\nu \gtrsim 100$  GeV) from various sources of which only a few might be resolved by directional information. The unresolved *diffuse* (or isotropic) neutrino flux is of vital interest as well as it could reveal sources typically associated with very distant and energetic astrophysical objects such as AGNs, GRBs and even first signs for new physics beyond the Standard Model (see [4, 5] for a review of current models).

However, the diffuse flux must be observed above the background of atmospheric neutrinos. The so called conventional atmospheric neutrino flux from pion and kaon decay produced in cosmic ray interactions in the atmosphere falls steeply with energy ( $\frac{dN}{dE_\nu} \propto E_\nu^{-\gamma}$ ,  $\gamma \approx 3.7$  for  $E_\nu \gtrsim 10$  TeV). At higher energies  $\mathcal{O}(10^5)$  GeV the contribution of neutrinos from the prompt decay of charmed mesons will begin to dominate the flux, thereby hardening its spectral index to  $\gamma \approx 2.7-3.0$ . The neutrino contribution from charm decay is yet unobserved and predictions vary by more than one order of magnitude. A measurement would allow to infer the cross-section for production of charmed particles.

Hence there are a number of interesting potential contributions to the diffuse flux of high energy neutrinos. In this paper we address the question under which conditions the different contributions can be resolved in future measurements. A Likelihood function is constructed incorporating both observable energy and angular information as well as systematic uncertainties of the background. The information content of future measurements is then analyzed by means of the Fisher matrix technique. We confirm the well know fact, that a cubic kilometer sized detector such as IceCube has a large discovery potential. However, at the same time we show that it also has a significant discrimination potential with respect to the various models. We analyze the information content contained in the various detection channels, namely the cascade- and muon-channels, and show what can be gained from their combination.

This paper is organized as follows. In the next section the various fluxes, experimental detection channels as well as the simulation of event rates are being discussed. In section 3 we review the Fisher matrix method and present its implementation with respect to the problem at hand. In section 4 we show the results of this analysis for a number of different cases. We conclude with a discussion of the results and compare to previous work done on similar subjects.

## 2. Simulation

The following fluxes will be considered in various combinations throughout the paper.

- An astrophysical flux of neutrinos:  $dN/dE = \alpha_{\text{agn}} \times E_{\nu}^{-\gamma_{\text{agn}}}$ . The slope  $\gamma_{\text{agn}}$  as well as the normalization  $\alpha_{\text{agn}}$  are treated as unknown parameters. The assumed true value for the slope is  $\gamma_{\text{agn}} = 2$  while  $\alpha_{\text{agn}}$  is allowed to vary from  $10^{-9}$  to  $10^{-7} \text{ cm}^{-2}\text{s}^{-1}\text{sr}^{-1}\text{GeV}^{-1}$ . The upper limit is chosen slightly below present experimental upper bounds [6, 7, 8, 9]. The Waxman-Bahcall (WB) upper bound [10] (see also [11]), which is of significant astrophysical relevance, corresponds to  $\alpha_{\text{agn}} = 4 \times 10^{-8} \text{ cm}^{-2}\text{s}^{-1}\text{sr}^{-1}\text{GeV}^{-1}$ . Neutrino oscillations will result in approximate equipartition of the total neutrino flux among all flavors [12].  $\alpha_{\text{agn}}$  refers to the normalization of the flux of one flavor.
- A flux of neutrinos from charm decay in the atmosphere. This flux is approximated by a power-law spectrum with  $\gamma_{\text{charm}} = 2.8$ . The normalization  $\alpha_{\text{charm}}$  ranges from  $10^{-5}$  to  $10^{-3} \text{ cm}^{-2}\text{s}^{-1}\text{sr}^{-1}\text{GeV}^{-1}$ , reflecting the range of available models around 100 TeV neutrino energies [13, 14, 15]. Although the shape of the spectrum is generally rather well predicted, small variations arise for example from the use of different cross-section parameterizations. Hence we again leave both normalization and slope as free parameters. A similar flux is assumed for  $\nu_e$  and  $\nu_{\mu}$  with no contribution from  $\nu_{\tau}$ .
- The atmospheric neutrino flux. Here we use a selected model [16] and we do not assume any free parameters. It was shown that the uncertainty in the flux prediction degrades the ability to detect additional flux contributions [17]. A 15% systematic uncertainty in the normalization is assumed [18]. The normalization is allowed to vary as a function of energy with a correlation length of one decade in energy. The assumed correlation in energy of the uncertainty reflects the fact that relevant ingredients of the calculations, as for example the cosmic ray composition or the interaction cross-sections of mesons in the atmosphere, are not anticipated to show sudden unaccounted variations. Hence in an experiment, the systematic uncertainties between two neighboring energy bins is correlated. The implementation of this correlated uncertainty is discussed in section 3. Note that neutrino oscillations have a very small effect on the atmospheric neutrino flux, due to the high energies considered here.
- The atmospheric muon flux. An analytical parameterization was used [19], which even at energies of  $10^7$  GeV agrees within a factor of two with a full CORSIKA Monte Carlo simulation [20]. The flux of atmospheric muons at the energies of interest ( $> \text{PeV}$ ) is less well predicted, because of the high energies involved. We assume an uncertainty of 50 %, again with a correlation length of one decade in energy.

Neutrino events ranging from  $10^3$  to  $10^{11}$  GeV are simulated using the Monte-Carlo simulation program ANIS [21]. ANIS allows generating  $\nu$ -events of all flavors, propagates them through the Earth and finally simulates  $\nu$ -interactions within a specified volume. All relevant Standard Model processes, i.e. charged current (CC) and neutral current (NC)  $\nu N$ -interactions as well as resonant  $\bar{\nu}_e - e^-$  scattering are implemented. Neutrino

regeneration as expected in NC-scattering,  $\nu + N \rightarrow \nu + X$ , and in  $\tau$  production and decay chains,  $\nu_\tau + N \rightarrow \tau + X$ ,  $\tau \rightarrow \nu_\tau + (\nu_i) + X$ , are included at all orders. The density profile of the Earth is chosen according to the Preliminary Earth Model [22]. Deep inelastic  $\nu - N$ -cross-sections were calculated in the framework of perturbative QCD (pQCD). Parameterization of the structure functions were chosen according to CTEQ5 [23], with logarithmic extrapolations into the small- $x$  region. Tau decay was simulated using the TAUOLA program [24].

The muon energy after propagating a distance  $X$  is approximated by:  $E_\mu = (E_{\mu,0} - a/b)e^{-bX} - a/b$ , with  $a = 3 \text{ MeVg}^{-1}\text{cm}^2$  and  $b = 4 \times 10^{-6} \text{ g}^{-1}\text{cm}^2$  [19]. Note that we are neglecting the fluctuations in muon range leading to slightly over-optimistic sensitivities for muons.

An IceCube-like detector is simulated. It is embedded in ice at a depth of 2 km with a bedrock starting in 3 km depth. We define three classes of events, all of which have been used by the AMANDA collaboration to search for a diffuse flux of neutrinos: cascades, upgoing muons and downgoing muon events. These classes are explained below.

- *Cascade* events which consist of electro-magnetic or hadronic cascades (also named showers). The particle cascade is localized in space and hence can only be observed near or within the detector volume. Charged current  $\nu_e$  and  $\nu_\tau$  interactions as well as NC interactions of any neutrino flavor lead to cascade-like events. In case of NC interactions, the visible energy is just a fraction of the incoming neutrino energy. In case of a CC tau neutrino interaction the vertex cascades and the cascade obtained from tau decay are spatially separated [25]. It is not yet established under which conditions and at which energy this *double bang* signature can be experimentally resolved, hence tau neutrino identification will not be assumed.

A main advantage of the cascade channel is the reduced background of atmospheric muons. An analysis performed with AMANDA has shown that for this class of events an almost uniform directional sensitivity can be reached [6, 26]. This leads to an improved sensitivity at higher energies, where Earth absorption effects become relevant. It is assumed that the background of atmospheric muons, due to their different event topology, can be totally eliminated above 1 TeV cascade energies.

- *Upgoing muon* events from CC  $\nu_\mu$  interactions producing an energetic muon transversing the detector. These events are selected by a zenith angle cut,  $\theta > 90^\circ$ , to eliminate the background of atmospheric muons. This is the traditional observation mode. The vertex of such muon events can be many kilometers away, hence the event rate for this class of events is generally higher than in the case of cascades. A further advantage is that for these events an angular resolution of about 1 degree can be achieved [2]. At high energies, neutrino absorption reduces the event rates in this channel significantly.
- *Downgoing muon* events from CC  $\nu_\mu$  interactions do not suffer of absorption in the Earth, hence they allow to extend the sensitivity of the instrument to *ultra high*

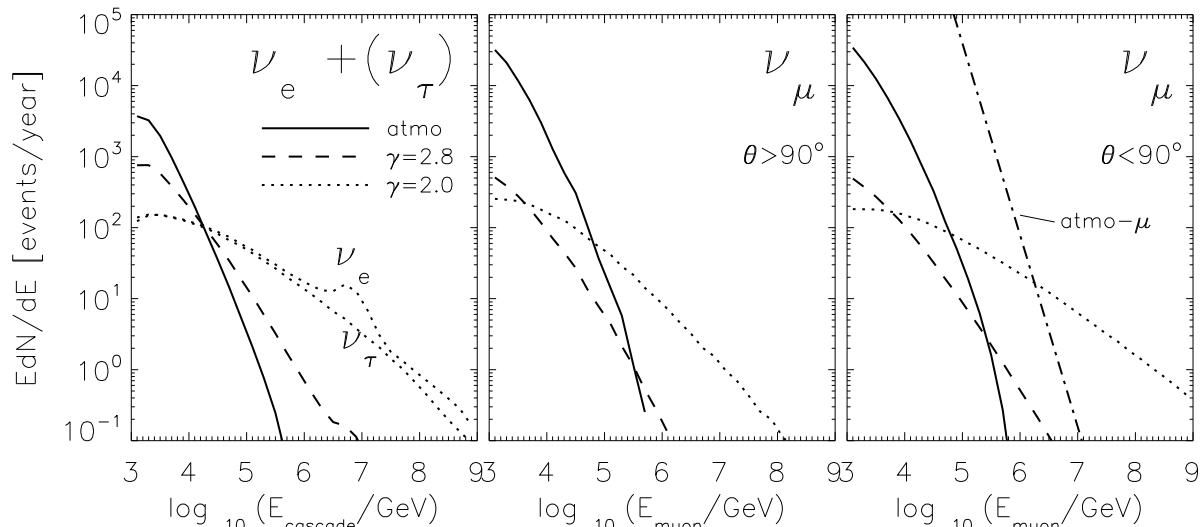


**Figure 1.** Observable energy spectrum at the detector site. An energy resolution of  $\sigma_{\log E} = 0.2$  was assumed. Left: The cascade energy released by electron neutrino interaction within a  $1 \text{ km}^3$  sized detector for three different input spectra and averaged over all directions. Also shown is the contribution expected from tau neutrinos with a flux similar to that of  $\gamma = 2$  electron neutrinos. Middle: The upgoing muon event rate as a function of the muon energy at the detector. A detection area of  $1 \text{ km}^2$  was assumed. Right: The downgoing muon event rate as a function of the muon energy at the detector. Additionally shown is the event rate due to atmospheric muons. The two input power-law spectra have slopes of  $\gamma = 2.0(2.8)$  and normalizations  $\alpha = 4 \times 10^{-8}(5 \times 10^{-4}) \text{ cm}^{-2} \text{ s}^{-1} \text{ sr}^{-1} \text{ GeV}^{-1}$ .

energies beyond  $10^9 \text{ GeV}$  [8, 20]. The disadvantage of this channel is that there is a large background of atmospheric muons. Therefore the effective energy threshold of this channel is  $10^6 - 10^7 \text{ GeV}$ . Here we will assume that the direction of these events can be reconstructed with a resolution of better than  $5^\circ$ . This is not yet achieved for AMANDA, however the large increase in size and modern readout technology should easily allow IceCube to achieve this resolution.

The resulting event rates are shown as a function of the observable energy in figure 1. The left plot shows event rates for electron neutrinos for different input spectra. Also shown are event rates for tau neutrinos from an astrophysical flux with  $\gamma_{\text{agn}} = 2.0$ . The “bump” around  $6 \times 10^6 \text{ GeV}$  is due to resonant  $\bar{\nu}_e - e^-$  scattering. For the highest energies the rate of tau neutrinos drops below that of electron neutrinos. That is because of the increasing tau decay length. The tau decays more frequently outside (“behind”) the detector, hence it does not contribute to the visible energy. The middle plot show the event rates for upgoing neutrino-induced muons as a function of the muon energy in the detector. The right plot show the event rates for downgoing neutrino-induced muons as well as for atmospheric muons.

An energy resolution of  $\sigma_{\log E} \approx 0.2$  for all event classes is assumed. Current algorithms used for the operating AMANDA detector are already achieving this resolution for cascade-like events [6, 26]. For muon events this is a mild extrapolation

of the currently obtained resolution:  $\log E_\mu \approx 0.3$  [29, 30]. However, the results of this work are not very sensitive on the exact value of the energy resolution.

### 3. The Method

One of the most popular and powerful methods for parameter estimation is the *maximum Likelihood method*, in which the parameters are determined by maximizing a Likelihood function  $L$  with respect to its parameters  $\vec{p}$ . Because of the low neutrino event rates, the appropriate Likelihood function is based on Poisson statistics:

$$L(\vec{p}) = \prod_i P(N_i | n_i(\vec{p})) = \prod_i \frac{N_i^{n_i} e^{-n_i}}{N_i!}, \quad (1)$$

where  $i$  is the index of the data bin,  $N_i$  is the number of observed events in data bin  $i$  and  $n_i$  is the number of events expected given the parameters  $\vec{p}$ . It is convenient to define the Log-Likelihood function as  $\mathcal{L} \equiv -\log L$  so that for the Likelihood function defined in Equation (1) one obtains:  $\mathcal{L} = -\sum_i N_i \ln n_i - n_i - \ln N_i!$ .

Here we are interested in the achievable accuracy of possible future measurements. To evaluate the sensitivity of the upcoming instruments one assumes a fiducial model, represented by  $\vec{p}$ , and analyzes the expected averaged constrains on the input parameters. However, there is more than one way to do this. One can simulate a future experiment in detail and then average over a large number of experimental outcomes by means of Monte Carlo technique. Such an approach produces very accurate results but at the same time it is computationally demanding and cumbersome in its implementation.

Here we chose a different method to calculate the sensitivity, namely the Fisher matrix method [27]. This method has become a popular tool in modern cosmology (see for example [28]), most likely due to its transparency and computational efficiency. Curiously, it is rarely used in the field of astroparticle physics. Hence we briefly review this method here (see [28] for a more in depth discussion of the method).

The Fisher information matrix is defined as the ensemble averaged Hessian matrix of the Log-Likelihood function evaluated at its minimum,

$$F_{ij} \equiv \left\langle \frac{\partial^2 \mathcal{L}}{\partial p_i \partial p_j} \right\rangle. \quad (2)$$

It represents the information content of the Likelihood function in the close vicinity of the true parameters. There are two important inequalities:  $\sigma_{p_i} \leq 1/\sqrt{F_{ii}}$ , a statement about the lower limit obtainable on the uncertainty  $\sigma_{p_i}$  on the parameter  $p_i$  in the case that all other parameters are exactly known. This theorem is known as the Cramér-Rao inequality. The second inequality is:  $\sigma_{p_i} \leq \sqrt{(F^{-1})_{ii}}$ , which is applicable in the case of all parameters being unknown (the parameters  $j \neq i$  are marginalized over). Here we will assume that  $\sigma_{p_i} = \sqrt{(F^{-1})_{ii}}$ , which is a reasonable approximation for well behaved Likelihood-functions.

For the Poisson based Likelihood function (1), one obtains the simple expression:

$$F_{ij} = \sum_k \frac{1}{n_k} \frac{\partial n_k}{\partial p_i} \frac{\partial n_k}{\partial p_j} \quad (3)$$

Note that so far only statistical errors have been assumed. What follows is an attempt to incorporate anticipated systematic uncertainties in the background prediction. We assume that the conventional atmospheric neutrino flux normalization at all energies is known with a precision of  $\sigma_{\text{atmo}} = 15\%$  [18], and that this uncertainty has a correlation length of one decade in energy. The uncertainty alters the neutrino event rate prediction  $n'_i = (1 + \eta_i)n_i$ , where  $\eta_i$  is a nuisance parameter reflecting the systematic uncertainty. Its probability function, which needs to be multiplied with the right hand side of Equation (1), is assumed to be Gaussian:

$$P(\vec{\eta}) \propto e^{-\vec{\eta}^T C \vec{\eta}} \text{ with } C_{ij} = \frac{1}{2\sigma_{\text{atmo}}^2(1 + |\log(E_i/E_j)|)^2}. \quad (4)$$

The dimension of the Fisher matrix increases by the number of nuisance parameters. Assigning the indices  $i, j$  to the physical parameters of interest (e.g. flux normalization or spectral slope) and  $\rho, \eta$  to the nuisance parameters, one obtains the following additional Fisher matrix elements:

$$F_{\rho\eta} = \sum_k C_{\rho\eta} + \delta_{\rho\eta} \frac{(n_k^{\text{atmo}})^2}{n_k} \text{ and } F_{i\delta} = \sum_k \frac{n_k^{\text{atmo}}}{n_k} \frac{\partial n_k}{\partial p_i}. \quad (5)$$

#### 4. The sensitivity

As described in section 2, we assume a neutrino flux composed of three components:

$$\phi(E_\nu) = \phi(E_\nu)_{\text{atmo}} + \alpha_{\text{agn}} E^{-\gamma_{\text{agn}}} + \alpha_{\text{charm}} E^{-\gamma_{\text{charm}}}, \quad (6)$$

with  $\gamma_{\text{agn}}, \gamma_{\text{charm}}, \alpha_{\text{agn}}$  and  $\alpha_{\text{charm}}$  being the free parameters of interest. Additionally there is a flux of atmospheric muons, which is the relevant background for the downgoing muon channel.

For this analysis the data was binned in energy-bins of the size of the energy resolution:  $\Delta \log E = 0.2$ . It was found that for the cascade and upgoing muons channel, there is little sensitivity increase when binning the data in energy *and* zenith angle direction. However, in the case of downgoing muons, the sensitivity generally increases by about a factor of two, if the reconstructed zenith angle is used as additional information (with bins of  $\Delta \cos \theta = 0.1$ ). This is because of the increase in overburden towards horizontal directions. The background of atmospheric muons decreases fast towards the horizon, while the signal rate increases due to increased target material. Hence for the downgoing muon channel explored in this work, the additional directional information is being used.

Figure 2 shows the significance  $\alpha/\sigma_\alpha = \alpha \sqrt{(F^{-1})_{\alpha\alpha}}$  with which the normalization  $\alpha$  can be measured as a function of  $\alpha$  assuming three full years of data. The various lines correspond to the different detection channels. The dotted line represents the combined measurement, where the corresponding Fisher matrix is<sup>‡</sup>  $F_{\text{combined}} = F_{\text{cascade}} + F_{\text{up-muon}} + F_{\text{down-muon}}$ .

<sup>‡</sup> Combining the individual Fisher matrices in a simple sum is only valid if there are no correlations between the channels. Certainly there will be some common systematic uncertainties, so the simple sum should be considered an optimistic assumption.

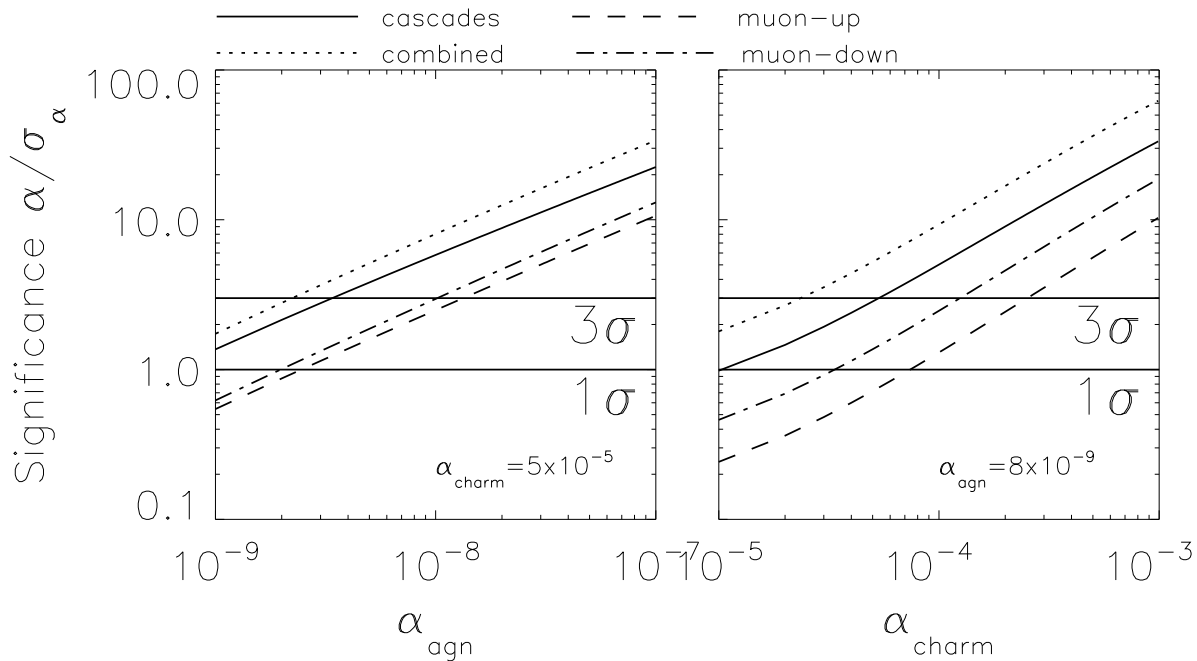


**Figure 2.** Significance (defined as  $\alpha/\sigma_\alpha$ ) of the measurement of  $\alpha$  as a function of  $\alpha$ . Left: The significance for  $\alpha_{\text{agn}}$  assuming an additional contribution of neutrinos from charm decay at the level of  $\alpha_{\text{charm}} = 5 \times 10^{-5} \text{cm}^{-2} \text{s}^{-1} \text{sr}^{-1} \text{GeV}^{-1}$ . Right: The significance of  $\alpha_{\text{charm}}$  assuming an extraterrestrial contribution with slope  $\gamma_{\text{agn}} = 2$  and normalization  $\alpha_{\text{agn}} = 8 \times 10^{-9} \text{cm}^{-2} \text{s}^{-1} \text{sr}^{-1} \text{GeV}^{-1}$ .

The left figure shows the significance of the extraterrestrial component with a charm contribution of strength  $\alpha_{\text{charm}} = 5 \times 10^{-5} \text{cm}^{-2} \text{s}^{-1} \text{sr}^{-1} \text{GeV}^{-1}$  while the right figure shows the significance of the measurement of the charm component with an assumed extraterrestrial contribution of strength  $\alpha_{\text{agn}} = 8 \times 10^{-9} \text{cm}^{-2} \text{s}^{-1} \text{sr}^{-1} \text{GeV}^{-1}$ .

These curves have a simple interpretation. We assume a measurement is called a discovery once the signal is established with  $3\text{-}\sigma$  significance (or in other words incompatible with zero at the 99.73 % level). One can read off the corresponding  $\alpha$  for which an ensemble of experiments will report a discovery. For smaller values of  $\alpha$  one will typically obtain only upper limits, while for larger values of  $\alpha$  a discovery becomes more significant.

As can be seen, a flux at the WB bound would be clearly detected in all three channels. The cascade channel, being most sensitive, will allow to make a detection at the  $\alpha = 6 \times 10^{-9}$  level, while the combined sensitivity still improves the results notably.

A flux of neutrinos from charm decay will be detected in all channels only for the highest of all normalizations. Here the cascade channel is significantly more sensitive allowing to detect a flux for  $\alpha_{\text{charm}}$  as low as  $5 \times 10^{-5} \text{cm}^{-2} \text{s}^{-1} \text{sr}^{-1} \text{GeV}^{-1}$ . However, in the presence of a significant flux of astrophysical neutrinos with spectral index  $\gamma \approx 2$ , it will become difficult to probe the lowest of all model predictions.

Note that a discussion on the expected uncertainties on the normalization itself becomes more complicated because of the strong covariance between the spectral shape



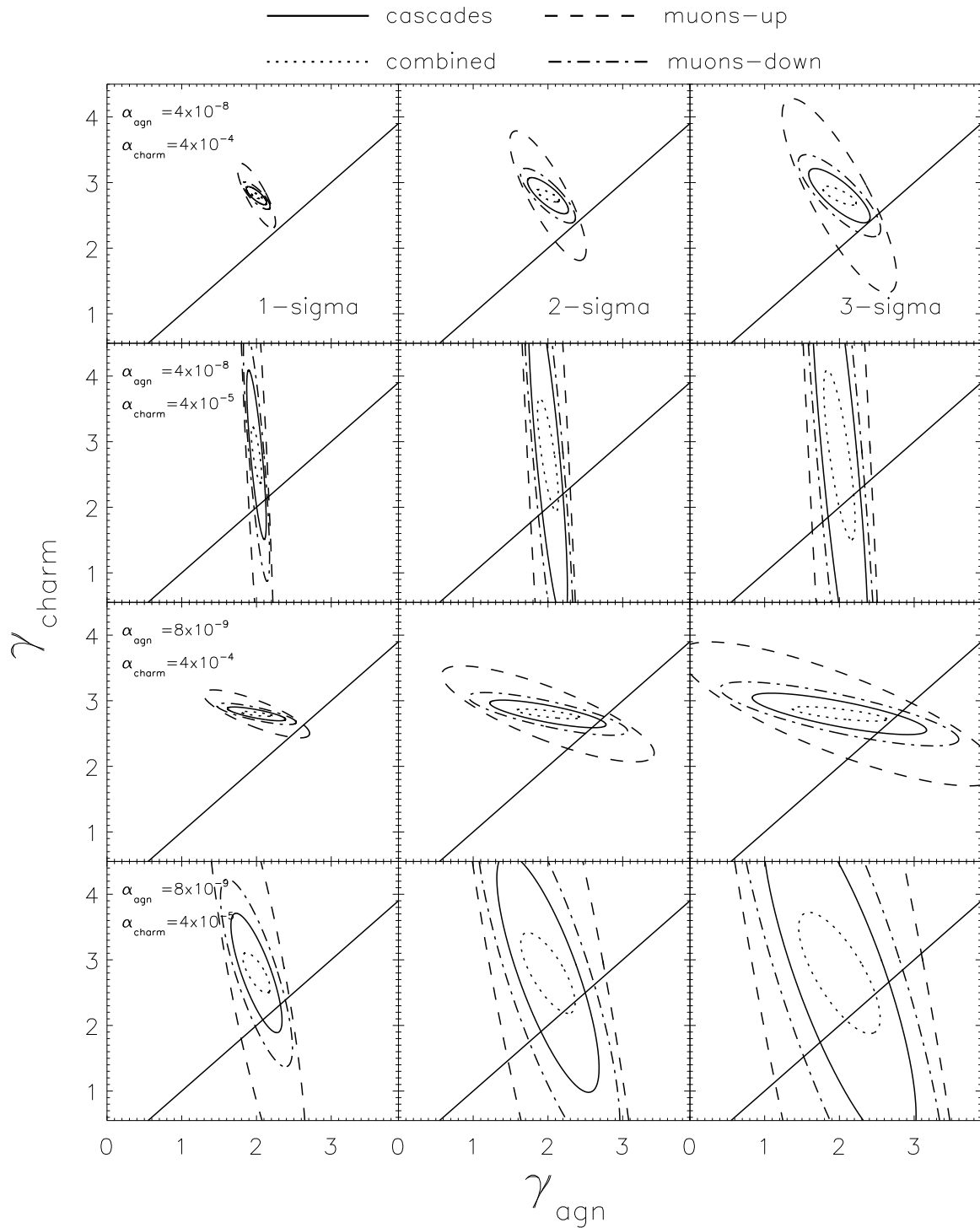


**Figure 3.** Averaged error ellipse in the  $\gamma_{\text{agn}} - \gamma_{\text{charm}}$  plane for the different channels. The columns from left to right show 1-, 2- and 3-sigma contours. The different rows show various combinations of flux normalizations. The diagonal lines represent  $\gamma_{\text{agn}} = \gamma_{\text{charm}}$ .

and the normalization  $\alpha$ . The covariance is large, since  $\alpha$  is defined for 1 GeV while

the relevant energy scale<sup>§</sup>  $E_s$  is 100 TeV to 1 PeV. Redefinition of the normalization to  $\alpha_s = \alpha E_s^\gamma$  would reduce the covariance. By presenting the sensitivity as  $\alpha/\sigma_\alpha$ , the results are independent of the energy scale assumed.

Once a signal has been established the shape of the underlying spectrum becomes of interest. Figure 3 shows the error ellipses in the  $\gamma_{\text{agn}} - \gamma_{\text{charm}}$  plane obtained for different combination of small/large extraterrestrial/charm fluxes. The normalization values used are  $\alpha_{\text{agn}} = (0.8 - 4) \times 10^{-8} \text{ cm}^{-2}\text{s}^{-1}\text{sr}^{-1}\text{GeV}^{-1}$  and  $\alpha_{\text{charm}} = (0.4 - 4) \times 10^{-4} \text{ cm}^{-2}\text{s}^{-1}\text{sr}^{-1}\text{GeV}^{-1}$ . The different columns show different significance contours ranging from 1- to 3-sigma (from left to right). The diagonal lines represent  $\gamma_{\text{agn}} = \gamma_{\text{charm}}$ . The interpretation of these ellipses are – within the framework of the Fisher matrix method – the following: Given the true values of  $(\alpha_{\text{agn}}, \gamma_{\text{agn}})$  and  $(\alpha_{\text{charm}}, \gamma_{\text{charm}})$ , future measurements of these parameters will be distributed according the probability contours.

In case the result of a measurement intersect the diagonal line, separation of the two components becomes impossible. As can be seen in the top row of the the figure, if both contributions are large, separation is possible at the 3-sigma level. If  $\alpha_{\text{agn}}$  is large, but  $\alpha_{\text{charm}}$  is small, only  $\gamma_{\text{agn}}$  can be meaningfully constrained. This is not surprising, considering that  $\alpha_{\text{charm}}$  has not yet been measured with 3-sigma significance. The other two combinations both show at most a 2-sigma separability of the two components. Again, of the individual channels it is the cascade channel which provides the tightest constrains.

## 5. Discussion

This paper gives an outlook on the sensitivity of future measurements of the diffuse neutrino flux. The primary detection channels used by AMANDA, which have proven capabilities [6, 8, 7], have been investigated and their sensitivity for measuring normalization and spectral shape of various potential fluxes was evaluated for a kilometer sized detector.

Thereby it was found that the cascade channel has the highest sensitivity. With three years of data, it should be possible to discover a flux of extraterrestrial neutrinos at a level as low as  $4 \times 10^{-9} E^{-2} \text{ cm}^{-2}\text{s}^{-1}\text{sr}^{-1}\text{GeV}^{-1}$ . It was found that the downgoing muon channel is rather sensitive, too, if in addition to muon energy the directional information is used. The traditional way to search for high energy neutrinos, namely by identifying upgoing muons, is least sensitive. This is because neutrino absorption in the Earth suppresses the observable neutrino spectrum at higher energies, therefore reducing significantly the lever arm needed to determine the spectral shape.

A combination of the individual channels leads to the largest sensitivity. Nevertheless, for confirmation it would be desirably to detect a significant signal in at least two of the three individual channels.

§ A representative energy scale can be defined as the weighted average of the energy of the bins, with the weights given by the bins contribution to the Fisher matrix.

A subset of the results presented here has been discussed previously. A detailed simulation of the muon channel for IceCube has resulted in precise estimates of the sensitivity to a single component diffuse flux [2]. However, spectral shape determination and the separability of an astrophysical flux contribution from a contribution from atmospheric prompt charm decay were not discussed. It was pointed out before that the cascade channel has a significant potential [14, 26, 17]. The ability to determine the spectral shape using the cascade channel was studied in Hooper *et al.* [17]. Because neutrino propagation in the Earth was not included in their simulation the analysis was restricted to downgoing cascades only. Further only CC interactions were taken into account. Finally the energy bins were chosen to be one order of magnitude, hence significantly larger than the energy resolution and bin size assumed here, reducing the sensitivity further. This list of differences explains why comparable sensitivities are obtained assuming only three years of data here while ten years of data was assumed in [17].

The work presented here is a first attempt to compare the various detection channels in a quantitative manner. Future analyzes might improve upon the sensitivities presented here. If tau neutrinos could be identified as such it would provide an important additional signature [31], as there is negligible background due to atmospheric tau neutrinos. Hence a single event would be a significant discovery. In practice the effective volume/area of an analysis is not confined to the geometrical one. For energetic – hence bright – events it could be larger, leading to higher sensitivities. Finally, one should restate that the analysis presented here assumes the availability of three years of data, while IceCube operation is planned for a time period of 10 years.

## Acknowledgments

The author would like to thank J. Beacom, T. Gaisser, T. Hauschildt and C. Spiering for helpful discussions and A. Gazizov for a fruitful collaboration on the ANIS program.

- [1] C. Spiering, Preprint arXiv:astro-ph/0503122.
- [2] J. Ahrens *et al.* [IceCube Collaboration], *Astropart. Phys.* **20**, 507 (2004).
- [3] P. Piattelli [NEMO Collaboration], *Nucl. Phys. Proc. Suppl.* **138** (2005) 191.
- [4] J. G. Learned and K. Mannheim, *Ann. Rev. Nucl. Part. Sci.* **50** (2000) 679.
- [5] F. Halzen and D. Hooper, *Rept. Prog. Phys.* **65** (2002) 1025.
- [6] M. Ackermann *et al.* [AMANDA Collaboration], *Astropart. Phys.* **22** (2004) 127.
- [7] J. Ahrens *et al.* [AMANDA Collaboration], *Phys. Rev. Lett.* **90** (2003) 251101.
- [8] M. Ackermann *et al.* [AMANDA Collaboration], *Astropart. Phys.* **22** (2005) 339.
- [9] J. Djilkibaev *et al.* [Baikal Collaboration], *Nucl. Phys. B Proc. Suppl.* **143** (2005) 335.
- [10] J. N. Bahcall and E. Waxman, *Phys. Rev. D* **64** (2001) 023002; J. N. Bahcall and E. Waxman, *Phys. Rev. D* **59** (1999) 023002.
- [11] K. Mannheim, R. J. Protheroe and J. P. Rachen, *Phys. Rev. D* **63** (2001) 023003.
- [12] H. Athar, M. Jezabek and O. Yasuda, *Phys. Rev. D* **62** (2000) 103007.
- [13] C. G. S. Costa, *Astropart. Phys.* **16** (2001) 193.
- [14] J. F. Beacom and J. Candia, *JCAP* **0411**, 009 (2004).
- [15] J. Candia and E. Roulet, *JCAP* **0309**, 005 (2003).

- [16] P. Lipari, *Astropart. Phys.* **1** (1993) 195.
- [17] D. Hooper, H. Nunokawa, O. L. G. Peres and R. Zukanovich Funchal, *Phys. Rev. D* **67** (2003) 013001.
- [18] T. K. Gaisser and M. Honda, *Ann. Rev. Nucl. Part. Sci.* **52** (2002) 153.
- [19] S. Eidelman et al. [Particle Data Group], *Phys. Lett.* **B592** (2004), 1.
- [20] S. Yoshida, R. Ishibashi and H. Miyamoto, *Phys. Rev. D* **69** (2004) 103004.
- [21] A. Gazizov, M. Kowalski, submitted to *Comp. Phys. Commun.*, Preprint arXiv:astro-ph/0406439.
- [22] see Ref. [83] in R. Gandhi et al., *Astropart. Phys.* **5** (1996) 81.
- [23] H. L. La et al. [CTEQ Collaboration], hep-ph/9903282;  
<http://www.phys.psu.edu/~cteq/>
- [24] S. Jadach et al., *Comput. Phys. Commun.* **76** (1993) 361.
- [25] J. G. Learned and S. Pakvasa, *Astropart. Phys.* **3** (1995) 267.
- [26] M. Kowalski, PhD Thesis, Humboldt University, Berlin (2003);  
<http://area51.berkeley.edu/manuscripts/>.
- [27] R.A. Fisher, *J. Roy. Stat. Soc.* 98 (1935) 39.
- [28] M. Tegmark, A. Taylor, A. Heavens, *Astrophys. J.* 480 (1997) 22.
- [29] H. Geenen et al. [AMANDA Collaboration], published in *Proc. of ICRC2003*, Tsukuba, Japan (2003).
- [30] P. Miocinovic, PhD Thesis, University of California, Berkeley (2001);  
<http://area51.berkeley.edu/manuscripts/>.
- [31] J. F. Beacom, N. F. Bell, D. Hooper, S. Pakvasa and T. J. Weiler, *Phys. Rev. D* **68**, (2003) 093005.